© 2015. Published by The Company of Biologists Ltd | Journal of Cell Science (2015) 128, 3781-3795 doi:10.1242/jcs.170969

RESEARCH ARTICLE

Essential role of endocytosis for interleukin-4-receptor-mediated JAK/STAT signalling

Kristina Kurgonaite[1,¶], Hetvi Gandhi[2,*,¶], Thomas Kurth[1], Sophie Pautot[1,‡], Petra Schwille[2,§], Thomas Weidemann[2,§,] and Christian Bökel[1,**]**

ABSTRACT

Many important signalling cascades operate through specialized signalling endosomes, but a corresponding mechanism has as yet not been described for hematopoietic cytokine receptors. Based on live-cell affinity measurements, we recently proposed that ligand-induced interleukin-4 receptor (IL-4R) complex formation and thus JAK/STAT pathway activation requires a local subcellular increase in receptor density. Here, we show that this concentration step is provided by the internalization of IL-4R subunits through a constitutive, Rac1-, Pak- and actin-mediated endocytosis route that causes IL-4R subunits to become enriched by about two orders of magnitude within a population of cortical endosomes. Consistently, ligand-induced receptor dimers are preferentially detected within these endosomes. IL-4 signalling can be blocked by pharmacological inhibitors targeting the actin polymerization machinery driving receptor internalization, placing endocytosis unambigously upstream of receptor activation. Taken together, these observations demonstrate a role for endocytosis that is mechanistically distinct from the scaffolding function of signalling endosomes in other pathways.

KEY WORDS: Cytokine receptor, Dimerization, IL-4, IL-13, IL-4Rα, IL-13Rα1, IL-2Rγ, JAK3, Pak1, Pak2, Rac1

INTRODUCTION

Endocytosis has traditionally been associated with the clearance of active receptors from the plasma membrane and hence signal downregulation. However, around 20 years ago it was shown, for different receptor tyrosine kinases (RTKs), that endocytosis of the activated receptor chains could control signal specificity and is required for the full activation of various downstream signal transducers (Di Guglielmo et al., 1994; Grimes et al., 1996; Vieira et al., 1996). Since then, positive contributions of endocytosis to the signal transduction process have also been identified for many other, unrelated signalling pathways (Bökel and Brand, 2014). Despite the molecular differences between these signal transduction cascades, several common themes have emerged at the cell biological level. For example, both for RTKs and TGF-β receptors, endosomal signalling is typically driven by clathrin-mediated endocytosis, whereas clathrin-independent internalization of the receptor chains is associated with degradation and signal downregulation (Di Guglielmo et al., 2003; Sigismund et al., 2008). Both these pathways also involve localized signalling from endosomes that act as platforms where receptors activated at the plasma membrane can interact with downstream pathway components (Miaczynska et al., 2004; Platta and Stenmark, 2011). However, similar endosomal signalling has also been observed in mechanistically unrelated signalling pathways such as the Toll-like receptor cascade (Kagan et al., 2008).

Here, we report that endocytosis is also strictly required for signal transduction from specific signalling endosomes in the interleukin-4 receptor (IL-4R) system. However, the underlying cell biological and biophysical principles differ from all other endocytosis-dependent signalling pathways studied to date.

The IL-4R is a typical representative of the class I cytokine receptor (CKR) family, which consists of single-pass transmembrane proteins that are non-covalently bound by cytoplasmic Janus kinases (JAKs) that contribute the enzymatic activity for signal transduction (Boulay et al., 2003; Nelms et al., 1999). With the exception of a small, homodimerizing group containing, for example, the erythropoietin receptor (Constantinescu et al., 2001) most class I CKRs form heterodimers (Weidemann et al., 2007). Formation of the active CKR heterodimers occurs in a two-step process, whereby the cytokine ligand first binds to one of the subunits that exhibits a higher ligand affinity. Subsequently, the second receptor chain is recruited into the complex by the occupied subunit (Whitty and Riera, 2008). Formation of these heterodimeric CKR complexes then triggers cross-activation of the cytoplasmic JAKs that in turn transform the CKR tails into docking sites for various downstream factors (Leonard and O'Shea, 1998). However, the subcellular compartment where these processes occur has as yet not been fully characterized.

CKRs can be grouped into families owing to the dimerization of different cytokine-specific high-affinity receptors with shared secondarily recruited subunits. When bound by IL-4, the IL-4Rα chain can recruit the IL-2Rγ chain (also called common γ-chain), which is also used by the high-affinity receptors for IL-2, -7, -9, -15, and -21, and is thus classified as a common γ-chain-using receptor (Boulay et al., 2003). This IL-4-induced heterodimer of IL-4Rα and IL-2Rγ is referred to as type 1 IL-4R complex. Alternatively, the IL-4-bound IL-4Rα subunit can recruit the IL-13Rα1 chain to form a type 2 complex, which is also induced when IL-13Rα1 bound by IL-13 recruits IL-4Rα (Nelms et al., 1999). Unusually among class I CKRs, the IL-4Rα chain can thus interact with two different cytokines to form three different, active receptor–ligand complexes (Fig. 1A). Generally, type 1 IL-4R signalling is restricted to cells of hematopoietic origin, whereas type 2 signalling is more widely distributed (Murata et al., 1998).

Both the interaction of IL-4 with its high-affinity receptor IL-4Rα and the subsequent recruitment of the IL-2Rγ chain have been

[1]Center for Regenerative Therapies Dresden (CRTD), Technische Universität Dresden, Fetscherstr. 105, Dresden 01307, Germany. [2]BIOTEC/Biophysics, Technische Universität Dresden, Tatzberg 47-51, Dresden 01307, Germany. *Present address: Institute IMAGINE, 24 Boulevard de Montparnasse, Paris 75015, France. ‡Present address: ITAV-CNRS USR3505, 1 Place Pierre Potier, 31106 Toulouse, France. §Present address: Cellular and Molecular Biophysics, Max Planck Institute of Biochemistry, Am Klopferspitz 18, Martinsried 82152, Germany. ¶These authors contributed equally to this work

**Authors for correspondence (weidemann@biochem.mpg.de; christian.boekel@crt-dresden.de)

Received 3 March 2015; Accepted 21 August 2015

Journal of Cell Science

Journal of Cell Science (2015) 128, 3781-3795 doi:10.1242/jcs.170969

characterized (Zhang et al., 2002a,b), and ectodomain crystal structures are available for all three ligand-induced heterodimers (Hage et al., 1999; LaPorte et al., 2008). Expanding on these *in vitro* studies, we have recently addressed IL-4R complex formation in the plasma membrane of living HEK293T cells (Gandhi et al., 2014; Weidemann et al., 2011). Surprisingly, we found that the affinities between fully occupied subunits are too low for efficient dimerization at endogenous plasma membrane expression levels by at least two orders of magnitude, implying the existence of a subcellular concentration mechanism that must act during signal transduction (Gandhi et al., 2014). In the course of these studies, we observed that IL-2Rγ–JAK3 complexes concentrate in a specific population of endosomes that are tightly associated with the cell cortex (hence termed cortical endosomes) (Gandhi et al., 2014). Trafficking of the IL-4R subunits to the cortical endosomes is constitutive and independent of ligand binding or pathway activity (Gandhi et al., 2014), consistent with previous observations in murine BaF3 cells (Friedrich et al., 1999). Following ligand stimulation, activated receptors are nevertheless preferentially associated with these cortical endosomes, suggesting a potential link between endocytosis and IL-4R signal transduction (Gandhi et al., 2014).

In the IL-2R context, IL-2Rγ is internalized through a unique Rac1- and Pak-regulated clathrin-independent endocytosis route (Grassart et al., 2008, 2010; Lamaze et al., 2001; Sauvonnet et al., 2005; Subtil et al., 1994) that appears to be highly related to the recently identified fast endophilin-mediated endocytosis (FEME) (Boucrot et al., 2014). Receptor internalization also involves the regulatory phosphoinositide 3-kinase (PI3K) subunit p85 and the large modular guanine-nucleotide-exchange factor (GEF) Vav2 (Basquin et al., 2013), although a role for these proteins in pathway activation has not been addressed.

Here, we show that the same endocytosis pathway plays a crucial role upstream of IL-4R signalling. We characterize cortical endosomes as the target compartment for this internalization step and show that constitutive enrichment of receptor subunits within the cortical endosomes constitutes a prerequisite for their efficient ligand-induced dimerization. Consistent with this, interfering with endocytosis by pharmacologically inhibiting the Rac1- and Pak-dependent actin polymerization machinery reversibly blocks IL-4R-mediated JAK/STAT signalling. Our proposed model of IL-4R pathway activation thus suggests a novel strategy for pharmacological manipulation of this important receptor class.

RESULTS

HEK293T cells as a model for IL-4R signalling

We recently introduced HEK293T cells as a model system to study the ligand-induced formation of fluorescently tagged IL-4R complexes, as their size and adherent growth makes them amenable to microscopy-based biophysical approaches (Gandhi et al., 2014; Weidemann et al., 2011). HEK293T cells endogenously express type 2 IL-4Rs, but not the type 1 components IL-2Rγ and JAK3 and the transcription factor STAT6 (Gandhi et al., 2014). Given that STAT6 activation strictly depends on the IL-4Rα receptor chain (Nelms et al., 1999), we chose phosphorylation of transfected STAT6 as a specific readout for JAK/STAT signalling. HEK293T cells expressing STAT6-transduced IL-4 transmit signals through their endogenous type 2 receptors, and this was suppressed by RNA interference (RNAi) against IL-13Rα1 (Fig. 1B). Signalling was also abolished by overexpression of a truncated signalling-dead IL-13Rα chain lacking the intracellular domain (IL-13Rα1-m356), which outcompetes the endogenous receptors and thus prevents signalling in response to either ligand (Gandhi et al., 2014) (Fig. 1C).

Following overexpression of wild-type IL-2Rγ and JAK3, STAT6 phosphorylation in response to IL-4 was normal (Fig. 1D). In contrast, IL-4 signalling was blocked by a truncated IL-2Rγ lacking the intracellular domain (IL-2Rγ-m271) (Gandhi et al., 2014) or by a JAK3 version carrying an engineered deletion of the kinase domain (JAK3-ΔJH1) (Hofmann et al., 2004) (Fig. 1D). Overexpression of IL-2Rγ and JAK3 therefore efficiently reroutes signalling to the type 1 pathway. Importantly, this did not prevent endogenous type 2 signalling in response to IL-13 stimulation (Fig. 1D). Thus, in the absence of ligand, even an excess of defective receptors did not affect the endogenous IL-4Rα chains, consistent with the negligible affinities between unoccupied IL-4R receptor subunits (Gandhi et al., 2014; LaPorte et al., 2008). Endogenous and overexpressed receptor chains therefore compete for the limiting pool of occupied IL-4Rα subunits. Accordingly, overexpression of IL-2Rγ and JAK3 rescued signalling suppressed by the truncated IL-13Rα1-m356 (Fig. 1E).

In summary, expression of different IL-4R subunits in HEK293T cells recapitulates the signalling output expected for both type 1 and type 2 IL-4R complexes, providing a convenient system for studying IL-4R signal transduction by both biochemistry and microscopy.

Endosomal localization of IL-4R subunits

While establishing this model, we previously confirmed that JAK3 and IL-2Rγ are mutually required for their recruitment to the plasma membrane from the cytoplasm and secretory pathway, respectively (Gandhi et al., 2014; Hofmann et al., 2004). However, instead of being smoothly distributed along the cell surface, the two molecules were found concentrated in speckle-like endosomal structures tightly associated with the cell cortex of transfected HEK293T cells (Fig. 1F–H; Fig. S1), which we termed cortical endosomes (Gandhi et al., 2014).

Fluorescence recovery after photobleaching (FRAP) experiments also demonstrated that there is negligible exchange between the cytoplasmic pool of JAK3 and the receptor-bound population associated with the cortical endosomes (Gandhi et al., 2014). Taken together with the absence of visible JAK3 membrane interactions in HEK293T cells (Fig. 1F), this makes the IL-2Rγ–(JAK3–eGFP) complex a suitable marker for the specific subpopulation of endosomes (Fig. 1G) in which we have found all three IL-4R subunits to be enriched at steady state (Gandhi et al., 2014). In contrast, directly labelling the IL-2Rγ chain with eGFP marked additional subcellular compartments, conceivably along the secretory or degradatory pathways (Fig. 1H).

To extend our previous observations using fluorescent fusion proteins (Gandhi et al., 2014), we characterized the endogenous endosomal protein complement of the cortical endosomes by immunofluorescence. The early endosomal proteins Rab5 (Fig. 2A) and EEA1 (Fig. 2B), as well as Rab11, a marker of the recycling compartment (Fig. 2C), were clustered in the vicinity of the cortical endosomes. When quantified using an object-based approach, 95.1±3.9% of the IL-2Rγ–(JAK3–eGFP) punctae exhibited an at least partial overlap with the similarly point-like Rab5 signals. A similar degree of association was observed for Rab11 (94.9±2.0%) and EEA1 (90.3±1.6%) but not for Rab7, a marker of late, degradatory endosomes (13.7±4.7%) (Fig. 2D) or the lysosome marker LAMP1 (12.4±8.4%) (results are mean±s.d., n=14 cells) (Gandhi et al., 2014).

These cortical endosomes formed without stimulation under conditions where STAT6 phosphorylation was undetectable (Fig. 1D), indicating that receptor subunit internalization does not require pathway activity. Consistent with this, Rab5-positive

Journal of Cell Science

Journal of Cell Science (2015) 128, 3781-3795 doi:10.1242/jcs.170969

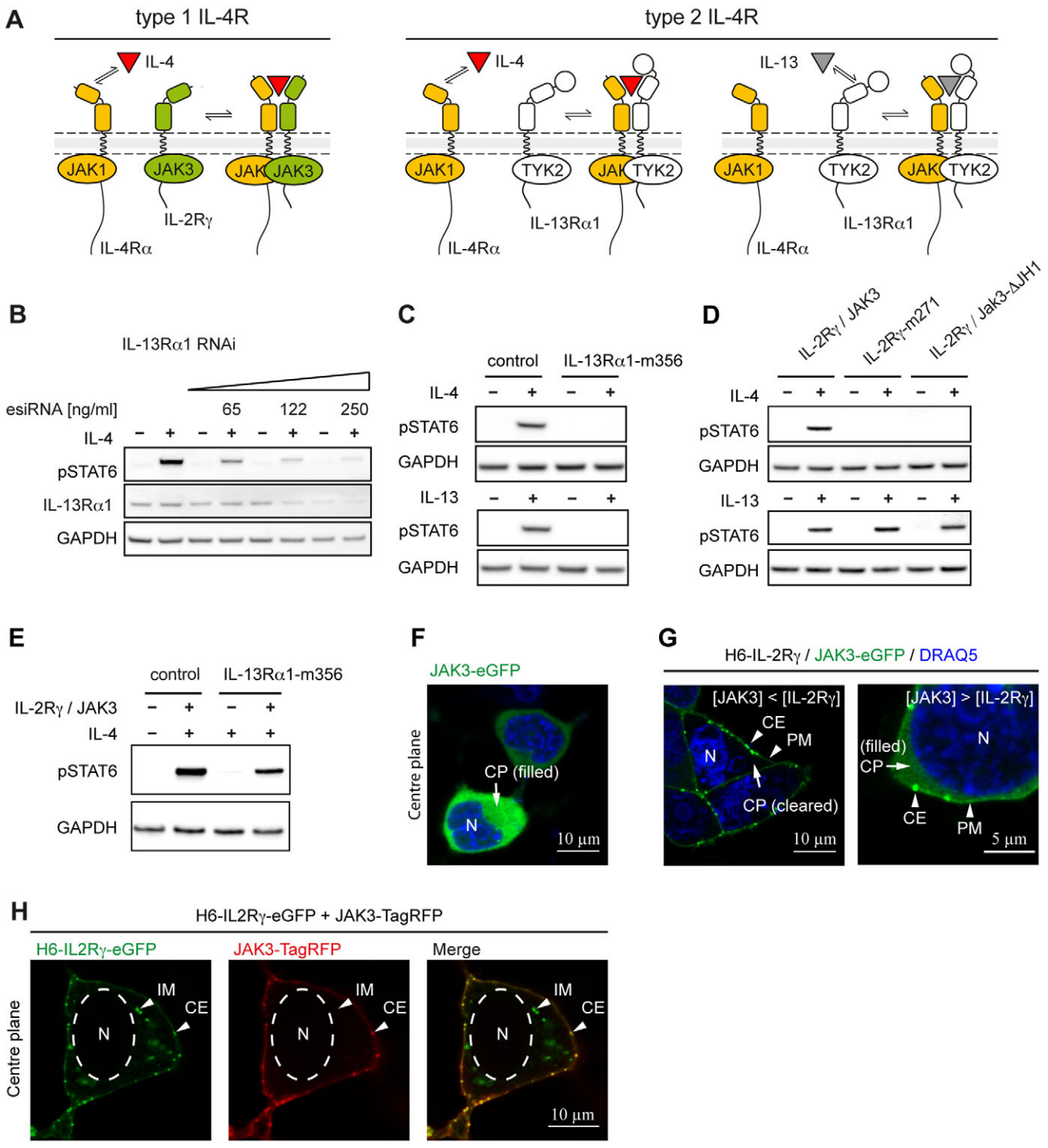

Fig. 1. HEK293T cells as a model for IL-4R signalling. (A) Schematic representation of IL-4R complex formation. (B) esiRNA-mediated knockdown of IL-13Rα1 in HEK293T cells inhibits endogenous type 2 IL-4R activity. (C) Overexpression of a truncated signalling-dead IL-13Rα1 receptor (IL-13Rα1-m356) abolishes type 2 IL-4R signalling in response to both IL-4 and IL-13. (D) Overexpression of the type 1 IL-4R components IL-2Rγ and JAK3–eGFP results in normal signal transduction. Signalling in response to IL-4, but not IL-13, is abolished by a truncated IL-2Rγ (IL-2Rγ-m271) or a kinase-dead JAK3 version (JAK3-D949N). (E) The signalling blockade caused by IL-13Rα1-m356 is overcome by an excess of IL-2Rγ and JAK3–eGFP. (F,G) Membrane recruitment of JAK3 by IL-2Rγ. (F) JAK3–eGFP transfected into HEK293T cells is fully cytoplasmic (CP) and excluded from the nucleus (N) regardless of expression level. (G) Co-transfection of IL-2Rγ induces recruitment of JAK3–eGFP to the plasma membrane (PM) and speckle-like cortical endosomes (CE). Cells expressing high levels of JAK3–eGFP exhibit both cytoplasmic and membrane-associated pools indicating binding site saturation. (H) IL-2Rγ–eGFP and JAK3–TagRFP colocalize at the plasma membrane and at cortical endosomes. Note internal membrane (IM) structures exclusively labelled by IL-2Rγ–eGFP. In B–E, phosphorylation of transfected STAT6 (pSTAT6) is the signalling readout and GAPDH is a loading control; F–H show central confocal sections.

Journal of Cell Science

Journal of Cell Science (2015) 128, 3781-3795 doi:10.1242/jcs.170969

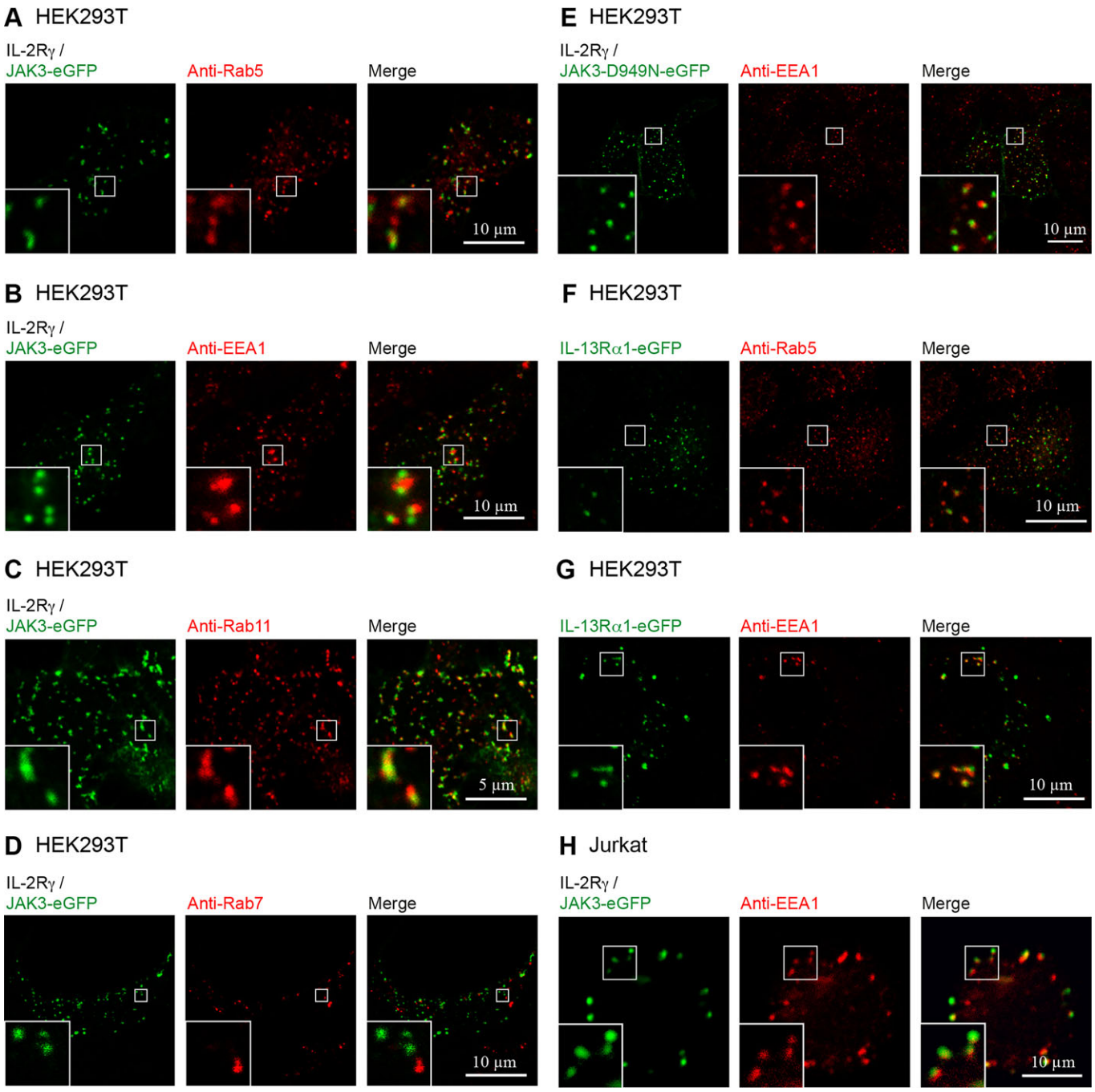

Fig. 2. Endosomal localization of IL-4R subunits. (A–E) Cortical endosomes marked by IL-2Rγ–(JAK3–eGFP) associate with the early endosomal markers Rab5 (A) and EEA1 (B), and the recycling endosomal marker Rab11 (C), but not with the late endosomal marker Rab7 (D). Rab5 also marks cortical endosomes formed by IL-2Rγ and the kinase-dead JAK3-D949N–eGFP (E). (F,G) Colocalization with Rab5 (F) and EEA1 (G) is also seen for the type 2 IL-4R subunit IL-13Rα1–eGFP. (H) EEA1 and JAK3–eGFP colocalize in Jurkat cells. All panels show surface section confocal images except H, which shows a central section.

cortical endosomes could also be observed when IL-2Rγ was co-expressed with JAK3-D949N–eGFP, an engineered kinase-dead JAK3 version (Hofmann et al., 2004) (Fig. 2E).

Pixel-wise colocalization analysis using the Manders correlation coefficients (Manders et al., 1993) confirmed this overall pattern: although the late markers exhibited no sign of colocalization with GFP-labelled cortical endosomes, Manders coefficients for GFP and Rab5, EEA1 and Rab11 indicated moderate colocalization (Table S1), consistent with a partial overlap between the signals. Given that the typical diameter of cortical endosomes labelled by IL-2Rγ and JAK3–eGFP (≈300 nm) (Gandhi et al., 2014) is relatively large for endosomal structures but still near the resolution limit of conventional laser scanning microscopy, we could not unambiguously resolve whether this close, but not fully overlapping, association reflects subdomains within individual cortical endosomes or a tight local clustering of separate endosomes.

Cortical-endosome-like structures partially overlapping with Rab5 (70.1±6.1%) (Fig. 2F) and EEA1 (77.1±6.4%) (Fig. 2G) also formed in HEK293T cells overexpressing the type 2 subunit

Journal of Cell Science

Journal of Cell Science (2015) 128, 3781-3795 doi:10.1242/jcs.170969

IL-13Rα1–eGFP, again mirrored by moderate pixel-wise colocalization (Table S1). These colocalization values are lower than for type 1 cortical endosomes, potentially reflecting partial localization of the tagged receptor to non-cortical endosome compartments, as also seen for IL-2Rγ–eGFP (Fig. 1H).

Finally, IL-2Rγ–(JAK3–eGFP) complexes exhibited a similar subcellular distribution in the T-lymphocyte-derived Jurkat cell line, which endogenously express the type 1 IL-4R (Fig. 2H). The observed partial overlap of 90.7±9.0% between the GFP-positive speckles and the EEA1 antibody signal was corroborated by moderate pixel-wise colocalization (Table S1). Thus, both in a lymphoid and a nonhematopoietic cell line, tagged subunits of the endogenous IL-4R subtype reside in punctate cortical endosomes.

Cortical endosomes are the site of IL-4R-mediated JAK/STAT signalling

We have previously shown that internalization of both IL-2Rγ and IL-4Rα into the IL-2Rγ- and JAK3-positive cortical endosomes is independent of ligand (Gandhi et al., 2014). We extended this here to both IL-4R types by tracking endocytosis of N-terminally His-tagged IL-4Rα by pulse–chase labelling with the hexahistidine-specific dye trisNTA–Alexa-Fluor-647 (Gandhi et al., 2014; Lata et al., 2006). At the 0-min time point, no vesicular structures were labelled regardless of ligand presence or IL-4R subtype (Fig. S2A–D). However, following the 20-min chase, most cortical endosomes of either subtype overlapped at least partially with a punctate Alexa Fluor 647 signal (Fig. S2E–H) (for quantification, see Table S2). Thus, for both IL-4R subtypes, IL-4Rα is constitutively internalized into endosomes that already contain its dimerization partner.

Accordingly, GFP-tagged IL-4Rα chains colocalize at steady state with cortical endosomes marked by IL-2Rγ–(JAK3–TagRFP) in the absence of ligand (Fig. 3A). However, specific immunostaining for activated IL-4Rα (pY497) was only observed following stimulation (Fig. 3B), when 83.3±5.2% (mean±s.d., n=5 cells) of the cortical endosomes overlapped at least partially with the phosphorylated (p)IL-4Rα signals, again reflected by moderate pixel-wise colocalization (Table S2). However, IL-4Rα–eGFP is prone to subcellular mislocalization artefacts (Gandhi et al., 2014). We therefore repeated the experiment by co-expressing non-labelled IL-4Rα with IL-2Rγ and JAK3–eGFP. In the absence of ligand, 8.6±4.6% of all cortical endosomes exhibited some overlap with a punctate signal in the pIL-4Rα channel (Fig. 3C), compared with 82.8±4.5% following stimulation with IL-4 (Fig. 3D), again with a concomitant increase in pixel-wise colocalization (Table S2).

The anti-pIL-4Rα antibody used above detects a phosphotyrosine (pY) involved in insulin receptor substrate (IRS)-1/2 signalling (Nelms et al., 1999). Even though activation of the IRS-1/2 and JAK/STAT pathways overall occur in parallel (Nelms et al., 1999; Weidemann et al., 2011), we therefore tested whether activated JAK1 (pY1022 and pY1023) and JAK3 (pY785) similarly colocalized in a ligand-dependent manner with type 1 cortical endosomes (Fig. 3E–H). In nonstimulated HEK293T cells transfected with IL-4Rα and IL-2Rγ–(JAK3–eGFP), 14.6±8.2% of the GFP-positive cortical endosomes overlapped at least partially with a phosphorylated JAK1 immunostaining signal (Fig. 3E) and 10.7±2.7% with activated JAK3 (Fig. 3G), potentially reflecting the low-level, ligand-independent activation observed after co-overexpression of functional IL-4R subunits (Gandhi et al., 2014). Stimulation with IL-4 increased these fractions to 88.1±5.5% (Fig. 3F) and 81.3±5.1%, respectively (Fig. 3H; see Table S2 for pixel-wise analysis). Like at the receptor level, activation of the downstream JAK/STAT branch thus appears biased towards the cortical endosomes.

Ultrastructural analysis of IL-4R subunit localization to cortical endosomes

Immunoelectron microscopy confirmed the tight apposition (average minimum distance 40 nm) of IL-2Rγ- and JAK3–eGFP-containing endosomes with the plasma membrane (Fig. 4A,B). Both in silver-enhanced anti-GFP nanogold stainings (Fig. 4A) and immunostainings with 10-nm gold particles (Fig. 4B), cortical endosomes appeared as multivesicular bodies (MVBs), with receptor subunits present both on the limiting membrane and intralumenal vesicles (Fig. 4A). Consistent with this, 97.9±1.9% of JAK3–eGFP-positive cortical endosomes exhibited partial overlap with the ESCRT-0 component Hrs, as assessed by confocal microscopy (Fig. 4C), an essential protein in MVB biogenesis (Bache et al., 2003), and 96.2±2.4% of all cortical endosomes also contained SARA (Fig. 4D, see Table S3 for pixel-wise colocalization analysis), a marker of signalling endosomes in the TGF-β and BMP pathways (Bökel et al., 2006; Tsukazaki et al., 1998).

These experiments confirmed that IL-2Rγ–(JAK3–eGFP) subunits are present within multivesicular cortical endosomes. However, the tendency to mislocalize when tagged with GFP (Gandhi et al., 2014) precluded using the same approach for IL-4Rα. Instead, we made use of the high-affinity ligand–receptor interaction with IL-4 (150 pM) (Zhang et al., 2002b) to determine the localization of endogenous IL-4Rα subunits relative to the IL-2Rγ- and JAK3–eGFP-marked cortical endosomes. Following validation by confocal microscopy (Fig. S2I,J), we therefore stimulated HEK293T cells expressing IL-2Rγ and JAK3–eGFP with biotin-labelled IL-4. After selecting regions of interest by analysing GFP immunofluorescence, we identified cortical endosomes within these areas based on their multivesicular ultrastructure and localization. Even though the endogenous cell surface levels of IL-4Rα are very low in most cells (1–10 receptors/μm^2) (Lowenthal et al., 1988; Ohara and Paul, 1987; Park et al., 1987), we could detect a specific localized signal (from 10-nm gold particles conjugated to protein A) for the biotinylated IL-4 within these putative cortical endosomes using an anti-biotin antibody (Fig. 4E).

IL-2Rγ–JAK3 complexes are enriched at cortical endosomes

Nanogold-tagged secondary antibodies can partially penetrate into sections, resulting in variable silver enhancement that precludes reliable quantification. We therefore quantified images obtained with protein A conjugated to 10-nm gold particles (Fig. 4B), which exclusively label epitopes exposed on the section surface. We focused on the cortical endosome limiting membrane, given that receptors on lumenal vesicles are isolated from the cytoplasm and thus, at least temporarily, unavailable for signalling. Quantification yielded on average 22.0±11.8 gold particles per endosome, 18.0±9.4 of which were associated with the limiting membrane (83.1±12.6%, mean±s.d., n=20 cells) (Table S4), translating into a linear density of 10.7±4.1 gold particles per μm of limiting membrane. In parallel, we separately quantified the density of anti-GFP immunogold particles at the plasma membrane directly overlying the cortical endosomes (3.98±1.57 gold particles per μm) and at the remainder of the plasma membrane elsewhere in the field of view (0.92±0.45 gold particles per μm). The density of gold-labelled anti-GFP particles per unit length in the cortical endosome limiting membrane was thus increased 14.0±7.6-fold relative to the

Journal of Cell Science (2015) 128, 3781-3795 doi:10.1242/jcs.170969

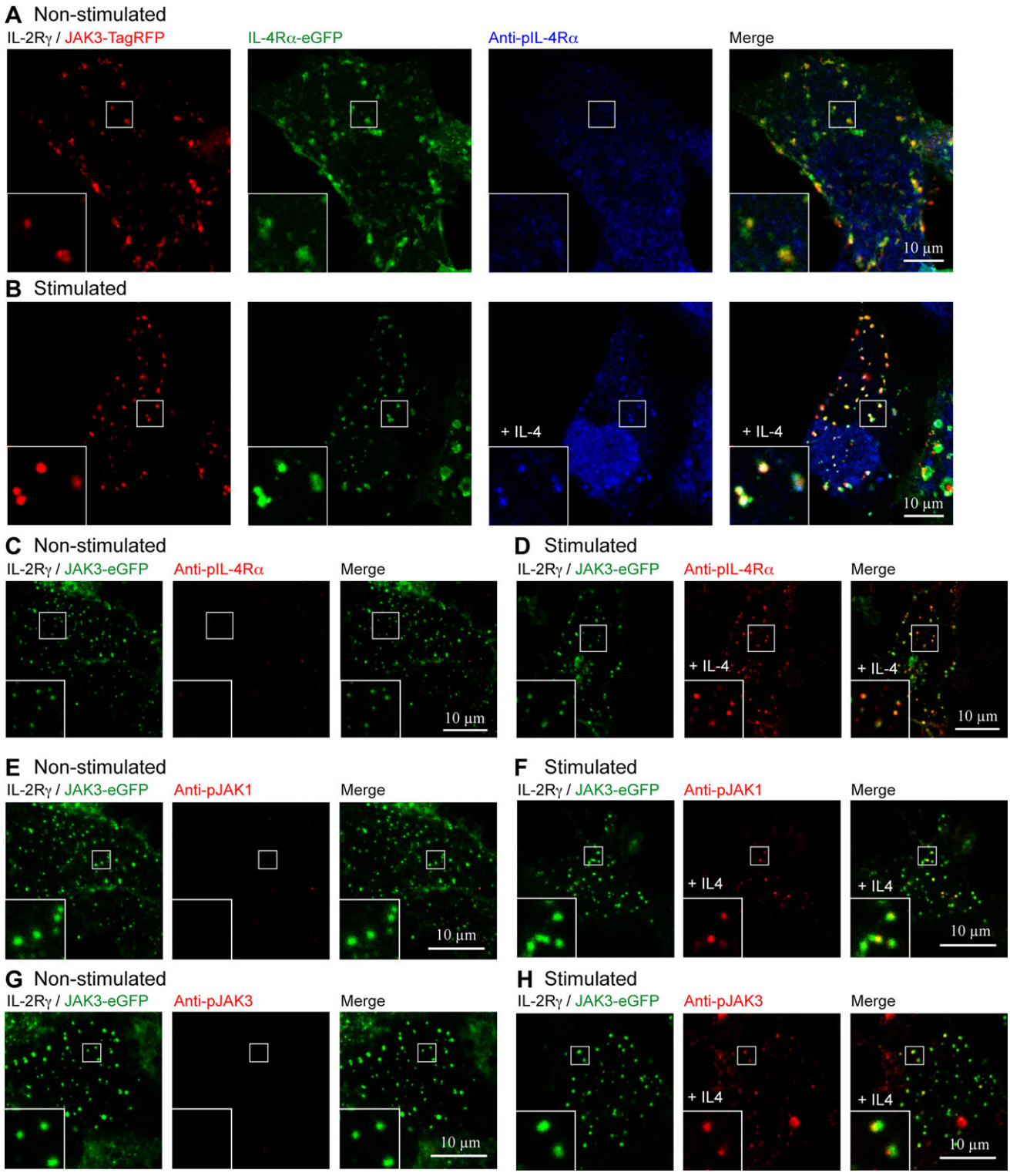

Fig. 3. Cortical endosomes are the site of IL-4R mediated JAK/STAT signalling. (A,B) HEK293T cells transfected with IL-2Rγ, JAK3–TagRFP and IL-4Rα–eGFP. The two type 1 receptor subunits colocalize in the absence of ligand (A). Following ligand stimulation (B), phosphorylated IL-4Rα (pIL-4Rα) becomes detectable at the cortical endosomes. (C–H) HEK293T cells transfected with IL-2Rγ and JAK3–TagRFP and unlabelled IL-4Rα. Markers for pIL-4R pathway components are largely absent from the cortical endosomes of unstimulated cells (C,E,G). pIL-4Rα (D), phosphorylated JAK1 (pJAK1) (F), and phosphorylated JAK3 (pJAK3) (H) become detectable at the cortical endosomes following IL-4 stimulation. All panels show surface confocal sections.

distant plasma membrane and 3.3±1.8-fold relative to the directly adjacent plasma membrane (Fig. 4F; Table S4). Given that receptor densities per area scale with the square of the densities per unit length, the local two-dimensional receptor concentrations in the limiting membrane of the cortical endosomes are increased by about 200-fold relative to the general plasma membrane. The order of magnitude of this concentration step is potentially sufficient to compensate for the inherently low affinities between the receptor subunits.

Journal of Cell Science

Journal of Cell Science (2015) 128, 3781-3795 doi:10.1242/jcs.170969

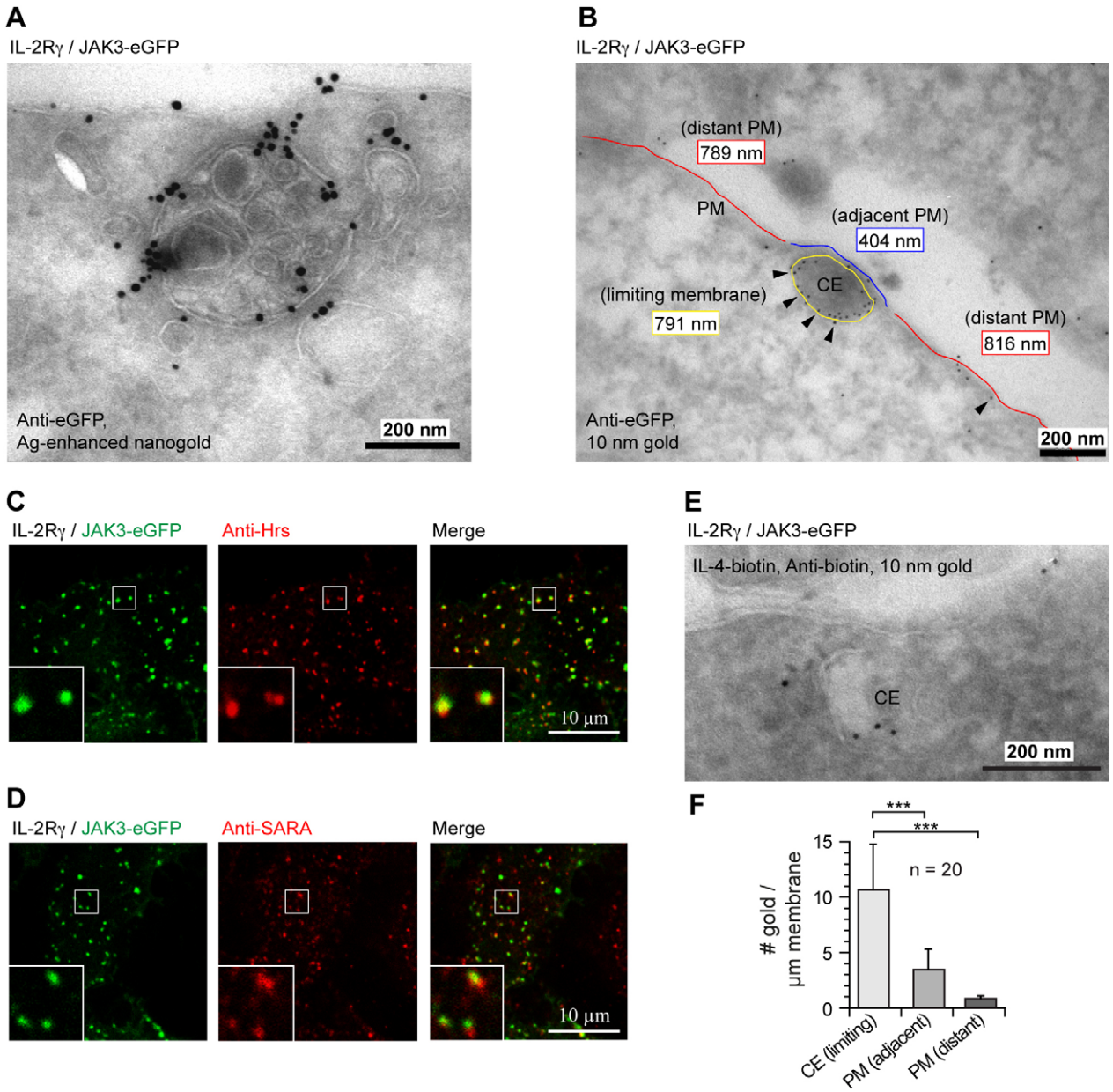

Fig. 4. Ultrastructural analysis and quantification. (A–E) HEK293T cells expressing IL-2Rγ and JAK3–eGFP. (A,B) Immunoelectron microscopy using anti-GFP antibody detected by silver-enhanced nanogold particles (A) and 10-nm immunogold particles (B) reveals accumulation of JAK3–eGFP at multivesicular cortical endosomes. PM, plasma membrane. (C,D) Cortical endosomes are marked by the MVB markers Hrs (C) and SARA (D). (E) Anti-biotin immunoelectron microscopy reveals the presence of biotinylated IL-4 within cortical endosomes (CE) selected by GFP fluorescence. (F) Quantification of 10-nm anti-GFP immunogold staining. At the cortical endosome limiting membrane, gold particles are enriched 3.3-fold relative to the adjacent plasma membrane and 14-fold relative to more distant membrane regions. Results are mean±s.d. C and D show surface confocal sections. ***P<0.01 (ANOVA).

Ligand-induced IL-4R heterodimerization preferentially occurs at the cortical endosomes

To visualize IL-4R complex formation directly, we used fluorescence lifetime imaging of Förster resonance energy transfer (FLIM–FRET) microscopy to track the subcellular distribution of IL-4R heterodimers carrying the CyPet fluorescence donor (IL-4Rα) or the YPet acceptor (IL-2Rγ or IL-13Rα1) within their cytoplasmic tails (Nguyen and Daugherty, 2005) (Fig. 5A).

In the absence of ligand, the IL-4Rα–CyPet donor-only lifetime was slightly higher at the plasma membrane (2.42±0.06 ns) in comparison with endosomes (2.32±0.07 ns; P<0.05) (Fig. 5B,C). Both values were weakly reduced by the presence of IL-4 (P<0.05). Introduction of either YPet-tagged acceptor subunit further reduced donor lifetime, potentially due to FRET caused by protein crowding and stochastic clustering. Consistently, this ligand-independent effect was especially noticeable in the cortical endosomes, where according to our confocal and electron microscopy data both subunits are constitutively enriched. Addition of IL-4 caused a significant shift towards even shorter lifetimes relative to each of these four different baselines, reflecting the ligand-induced formation of receptor heterodimers. For the low-affinity type 1 IL-4R complexes, this reduction was much more pronounced in endosomes (from 2.06±0.05 ns down to 1.57±0.06 ns in the presence of ligand, P<0.01) than at the plasma membrane (2.29±0.05 ns versus 2.18±0.07 ns, P<0.01). In contrast, under the same

Journal of Cell Science

Journal of Cell Science (2015) 128, 3781-3795 doi:10.1242/jcs.170969

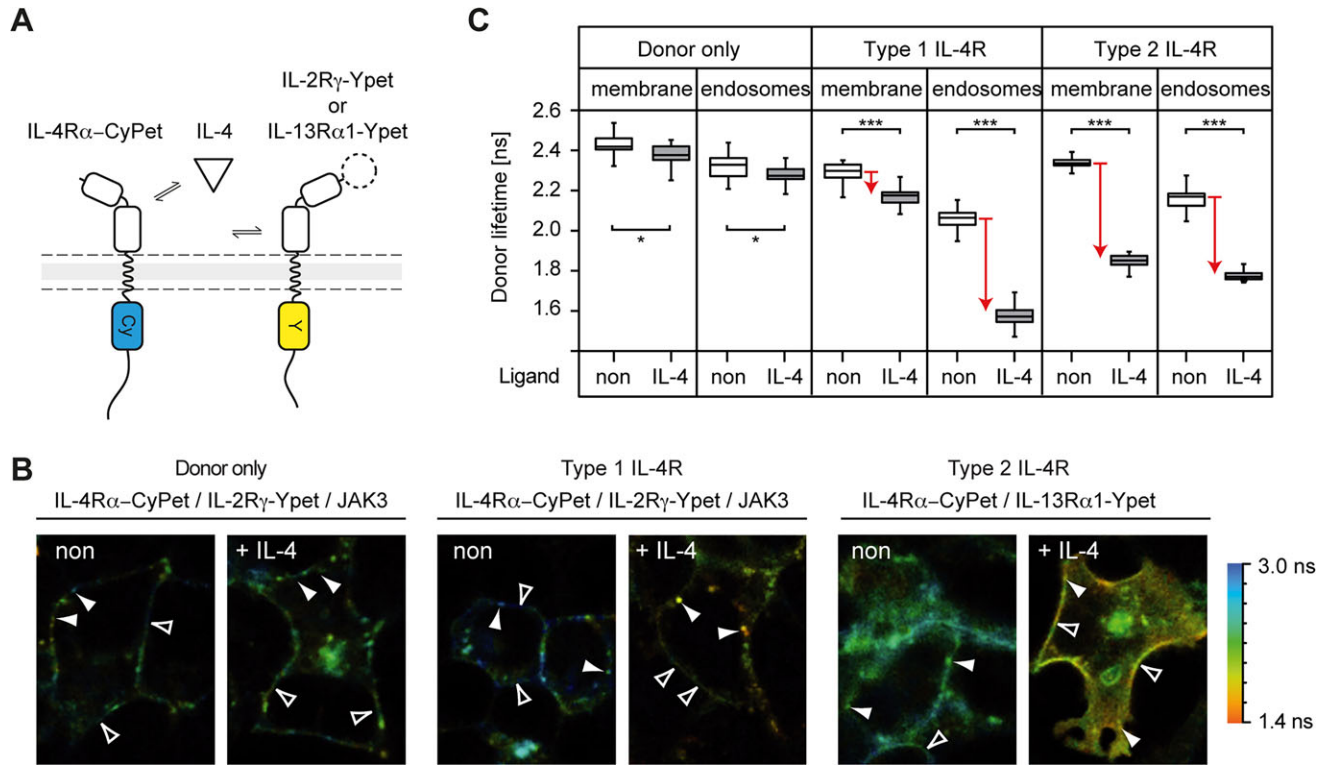

Fig. 5. Detection of receptor dimerization by FLIM. (A) Experimental strategy. FRET caused by ligand induced heterodimerization of CyPet (Cy)-tagged IL-4Rα and YPet (Y)-tagged IL-2Rγ or IL-13Rα1 reduces donor fluorescence lifetime. (B) FLIM images of HEK293T cells expressing IL-4Rα–CyPet in combination with nonfluorescent IL-2Rγ (donor only), IL-2Rγ–YPet or IL-13Rα1–YPet (acceptors). Homogeneous membrane area (open arrowheads) and cortical endosomes (arrowheads) as used for quantification. Colour indicates fluorescence lifetime (sidebar). (C) Quantification of FLIM measurements. IL-4 exposure shifts the donor lifetimes to lower values (red arrows). Type 1 IL-4R complexes preferentially form within cortical endosomes whereas type 2 IL-4 receptors also form at the plasma membrane. Box-and-whisker plots indicate the 2nd and 3rd quartile (box), median (horizontal line) and 1.5× interquartile range (whiskers). **P*<0.05, ****P*<0.01 (Student's *t*-test).

conditions the high-affinity type 2 IL-4R complexes were readily detected both within endosomes (2.16±0.06 ns versus 1.78±0.04 ns; $P<0.01$) and at the plasma membrane (2.34±0.04 ns versus 1.85±0.04 ns, $P<0.01$) (Fig. 5B,C).

These FLIM results confirm our previous fluorescence cross-correlation spectroscopy (FCCS) observations: at comparable expression levels (Gandhi et al., 2014), ligand-induced dimerization at the plasma membrane was readily detectable by FCCS for the higher affinity type 2 IL-4R, whereas dimers of the lower affinity type 1 IL-4R were just above detection threshold (Gandhi et al., 2014). The IL-4-induced lifetime shifts at the membrane thus correlate qualitatively with both the affinities governing formation of the respective receptor complexes (Gandhi et al., 2014) and their relative signalling strength (Gandhi et al., 2014; LaPorte et al., 2008).

In contrast, within the cortical endosomes the FLIM results indicate pronounced ligand-dependent heterodimerization for both receptor types. Thus, endocytic trafficking to the cortical endosomes facilitates efficient dimerization also for the low-affinity type 1 IL-4R complexes, potentially reflecting the increased local receptor concentrations detected by independent means.

IL-4R ligand and receptor subunits are internalized by a specific, Rac1-, Pak- and actin-dependent endocytosis route

The type 1 IL-4R and IL-2R complexes share IL-2Rγ, which in the IL-2R context is internalized by a specific actin-mediated and dynamin-dependent endocytosis route (Lamaze et al., 2001; Subtil et al., 1994). This pathway is regulated by the small GTPase Rac1 and its downstream kinases Pak1 and Pak2 that trigger local actin branching and polymerization (Sauvonnet et al., 2005). In agreement with this pathway also acting in our HEK293T model, most cortical endosomes overlapped with immunostaining against the activated phosphorylated form of the RacGEF Vav2 (Vav2-pY172, 95.7±3.9%, mean±s.d., $n=5$ cells) (Fig. 6A; Table S3), which has previously been implicated in IL-2R endocytosis (Basquin et al., 2013).

Consistently, 93.0±2.7% of all cortical endosomes colocalized with Arp2, a nucleation factor for actin branching (Fig. 6B), and cortical endosomes were surrounded by basket-like actin structures, potentially explaining their stable cortical localization (Fig. 6C). We confirmed this actin association by correlative light electron microscopy (CLEM) (Fig. S2K). Arp2 also colocalized with cortical endosomes containing the type 2 receptor subunit IL-13Rα1–eGFP (90.2±4.0%) (Fig. 6D, Table S3).

Even though the transferrin receptor is exclusively internalized by standard clathrin-mediated endocytosis, cortical endosomes could also be loaded with transferrin after a 5-min chase (Fig. S3A) as expected for regular Rab5-positive early endosomes.

Inhibition of IL-4R endocytosis blocks JAK/STAT pathway activation

To functionally link this endocytosis route with IL-4R signalling, we used pharmacological inhibitors for different endocytic pathways. Dynasore (Macia et al., 2006) was used to interfere with all dynamin-dependent endocytosis pathways, whereas EHT-

Journal of Cell Science

Journal of Cell Science (2015) 128, 3781-3795 doi:10.1242/jcs.170969

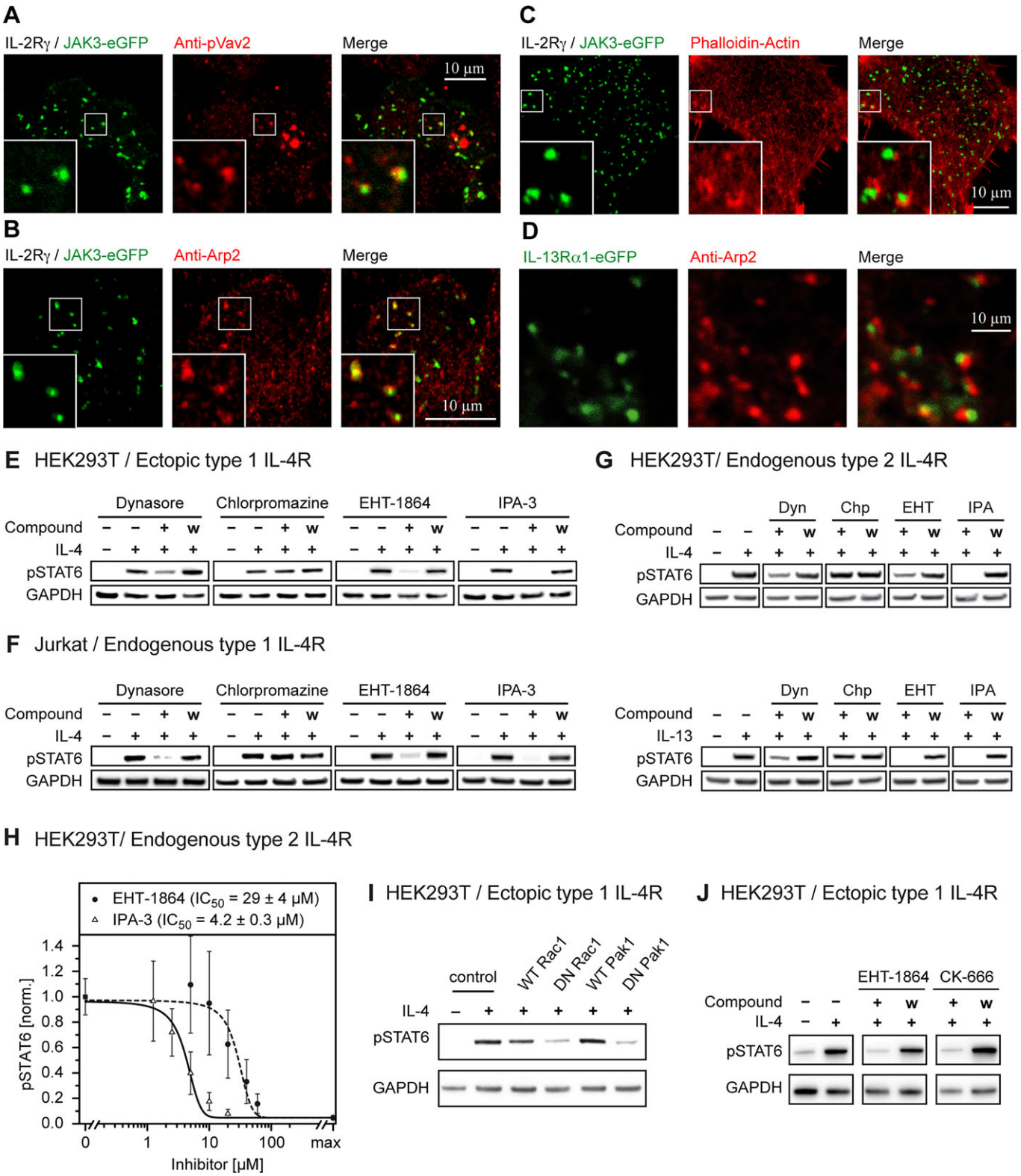

Fig. 6. Inhibition of actin-mediated endocytosis reversibly blocks IL-4R-mediated STAT6 phosphorylation. (A–C) Cortical endosomes marked by IL-2Rγ–(JAK3–eGFP) complexes colocalize with activated Vav2 phosphorylated at Y172 (pVav2) (A), Arp2 (B) and basket-like actin accumulations (C). Arp2 also decorates endosomes marked by IL-13Rα1–eGFP (D). (E–G) Inhibition of dynamin (dynasore, 320 µM), Rac1 (EHT-1864, 50 µM), Pak1 and Pak2 (IPA-3, 10 µM), and clathrin-mediated endocytosis (chlorpromazine, 7 µM). Dynasore, EHT-1864 and IPA-3 reversibly block type 1 IL-4R signalling in HEK293T cells overexpressing IL-2Rγ and JAK3 (E), endogenous type 1 signalling in Jurkat cells (F) and endogenous type 2 signalling in HEK293T cells in response to both IL-4 and IL-13 (G), whereas chlorpromazine has no effect (E–G). (H) Dose–response curves of IL-4R pathway inhibition by EHT-1864 and IPA-3 (four independent experiments per compound). Error bars denote s.d. (I,J) Inhibition of type 1 IL-4R signalling in HEK293T cells overexpressing IL-2Rγ and JAK3 by dominant-negative (DN) Rac1 (T17N) and Pak1 (K299R) (I) or the Arp2/3 inhibitor CK-666 (400 µM) (J). A–D show surface confocal sections; in E–J, phosphorylated STAT6 (pSTAT6) is the signalling readout and GAPDH is a loading control; w, compound washout; WT, wild type.

Journal of Cell Science

Journal of Cell Science (2015) 128, 3781-3795 doi:10.1242/jcs.170969

1864 (Shutes et al., 2007) and IPA-3 (Deacon et al., 2008) were used to block Rac1- and Pak-dependent pathways, respectively. Chlorpromazine (Wang et al., 1993) served as a control reagent targeting clathrin-mediated endocytosis, which was not predicted to affect CKR internalization (Subtil et al., 1994). As expected, dynasore and chlorpromazine, but not EHT-1864 and IPA-3, were able to block clathrin-mediated transferrin uptake (Fig. S3B) without affecting STAT6 expression (Fig. S3C).

Consistent with a role of Rac1- and Pak-mediated endocytosis in signalling, EHT-1864 and IPA-3 caused a strong but reversible reduction of ligand-dependent STAT6 phosphorylation in HEK293T cells with a reconstituted type 1 IL-4R (Fig. 6E). The influence of dynasore was consistent but somewhat weaker, whereas chlorpromazine had no effect. Signalling through the endogenous type 1 IL-4R of Jurkat cells (Fig. 6F) and endogenous type 2 signalling in HEK293T cells in response to both IL-4 and IL-13 (Fig. 6G) were equally affected. Thus, all three ternary IL-4R–ligand complexes require Rac1- and Pak-mediated endocytosis for productive JAK/STAT signalling. To further support this link we determined dose–response curves for the inhibition of endogenous type 2 IL-4R activity by EHT-1864 and IPA-3, allowing us to estimate an IC_{50} for STAT6 phosphorylation of 29±4 µM for EHT-1864 and 4.2±0.3 µM for IPA-3 (mean±s.d.) (Fig. 6H). Both values are roughly consistent with published IC_{50} values for these drugs in different systems [e.g. 12.5 µM for EHT-1864-induced cancer cell apoptosis (Hinterleitner et al., 2013) and 2.5 µM for inhibition of Pak1 kinase activity by IPA-3 (Deacon et al., 2008)].

Signalling through the reconstituted type 1 pathway was also reduced by dominant-negative Rac1 (D17N) (Kraynov et al., 2000) and Pak1 (K299R) (Sells et al., 1997) (Fig. 6I), confirming the pharmacological inhibition data. Finally, signalling was also inhibited by CK-666, a specific inhibitor of the Arp2/3 actin-branching complex (Hetrick et al., 2013) (Fig. 6J), demonstrating that it is the actin-organizing role rather than another output of the potentially pleiotropic Rac1 and Pak cassette that is required for IL-4R pathway activation.

Inhibition of the actin-dependent endocytosis pathway reduces ligand and receptor trafficking to the cortical endosomes

We finally quantified the effect of drug treatment on the uptake of ligand and receptor subunits to the cortical endosomes. HEK293T cells transfected with IL-4Rα1, IL-2Rγ and JAK3–eGFP were pretreated with compounds, and loaded at 4°C with a fully active Alexa-Fluor-647-labelled IL-4 (Fig. S4A) (Duppatla et al., 2014). Localization of the labelled IL-4 to the cortical endosomes was then monitored by quantitative confocal microscopy (Fig. S4B–D), either immediately (Fig. S4E,F) or after a chase of 20 min at 37°C in the presence of inhibitors (Fig. S4G,H). Cells treated with dynasore had to be excluded from this analysis, owing to a ubiquitous fluorescent background and the appearance of vesicular inclusions in the cytoplasm that precluded the measurement of ligand uptake relative to individual cortical endosomes. Given that we used unlabelled IL-4Rα, we limited our analysis to cells exhibiting robust surface labelling by the fluorescent ligand, which confirmed the presence of its high-affinity receptor (Fig. 7A–E).

Consistent with internalization occurring through clathrin-independent and Rac1-, Pak- and actin-mediated endocytosis, endosomal ligand levels were similar for the DMSO control and after chlorpromazine treatment (Fig. 7A,B). In contrast CK-666, EHT-1864, and IPA-3 (Fig. 7C–E) all caused a significant reduction in the average total amount of ligand fluorescence internalized into all cortical endosomes of a given cell (Fig. 7F) at concentrations validated for inhibition of signalling (Fig. S4I). Owing to the close apposition of cortical endosomes and plasma membrane, restricting the analysis to cells exhibiting visible surface labelling invariably lead to overestimation of endosomal ligand levels by projection effects, which was reduced by focussing on cortical endosomes near the bottom membrane (Fig. 7G).

Receptor internalization in the absence of ligand was tracked by a similar loading assay using pulse labelling of cells expressing N-terminally His-tagged receptor subunits with trisNTA–Alexa-Fluor-647 (Gandhi et al., 2014; Lata et al., 2006). Although nonspecific internalization of the trisNTA dye contributes ∼10% to the endosomal signals (Gandhi et al., 2014), uptake of H6-IL-4Rα and H6-IL-2Rγ into cortical endosomes following a chase of 10 min at 37°C was reduced to about 50% of control levels in the presence of EHT-1864 (Fig. 7H), again taking projection effects into account. Both assays thus provide conservative estimates of the true reduction in ligand and receptor uptake caused by the inhibitor treatment.

DISCUSSION

We have previously shown that individual IL-4R subunits diffuse freely within the plasma membrane (Gandhi et al., 2014; Weidemann et al., 2011). Following ligand binding to one subunit, we observed recruitment of a second subunit into heterodimers, consistent with the canonical view of IL-4R activation (LaPorte et al., 2008; Zhang et al., 2002a). However, our FCCS experiments demonstrated that the two-dimensional dissociation constants of the IL-4R complexes are of the order of several hundred to a thousand receptors per μm^2 (Gandhi et al., 2014). At endogenous IL-4R cell surface densities of 1–10 receptors per μm^2 (Lowenthal et al., 1988; Ohara and Paul, 1987; Park et al., 1987), the fraction of subunits entering active heterodimers would thus be negligible even with saturating ligand levels. Productive signalling therefore demands a subcellular concentration step that is missing from current models of CKR activation.

Based on the experiments described here, we therefore propose a revised model of IL-4R pathway activation, whereby endocytosis is an essential process upstream of receptor dimerization. According to this model, receptor subunits are continuously and constitutively endocytosed to a population of cortical signalling endosomes (cortical endosomes) and recycled to the plasma membrane, thus sampling the environment for presence of ligand (Fig. 8). Fine tuning of endocytosis and recycling rates establishes a steady state increase in receptor density in the limiting membrane of the cortical endosomes relative to the plasma membrane. This subcellular concentration step compensates for the low affinities between ligand occupied and secondarily recruited IL-4R subunits. Thus, in the presence of ligand endocytosis, the local formation of receptor heterodimers at the endosomes can occur, which would, according to the law of mass action, be disfavoured at endogenous plasma membrane densities. This unusual role of endocytosis for JAK/STAT pathway activation is supported by several lines of evidence as described below.

First, electron microscopy quantification revealed an increase in subunit density of around two orders of magnitude from the plasma membrane to the limiting membrane of the multivesicular cortical endosomes. Increasing endogenous receptor densities by the same factor would suffice to bring the resulting endosomal receptor densities into the range of the $K_{d,2D}$ values of the respective complexes, which is a prerequisite for efficient dimerization in response to ligand. Although our quantifications were performed on

Journal of Cell Science

Journal of Cell Science (2015) 128, 3781-3795 doi:10.1242/jcs.170969

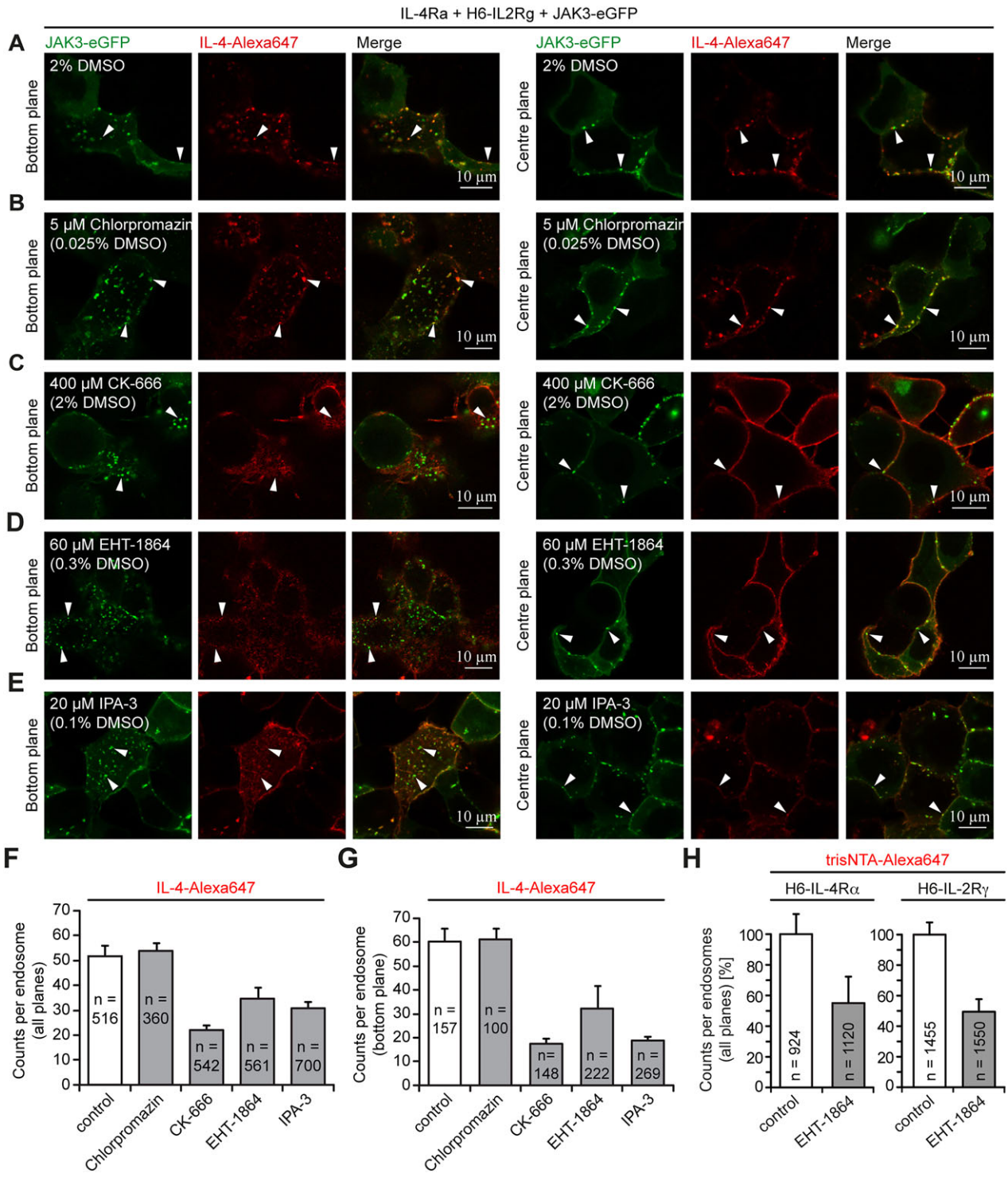

Fig. 7. Inhibition of actin-mediated endocytosis blocks ligand and receptor trafficking to cortical endosomes. (A–G) IL-4 loading assay. HEK293T cells expressing IL-2Rγ and JAK3–eGFP and preincubated with compounds at indicated concentrations were pulse-labelled on ice with IL-4–Alexa-Fluor-647. Following a 20-min chase at 37°C internalization of ligand into cortical endosomes was detectable in cells treated with 2% DMSO (vehicle control) (A) or chlorpromazin (B). Internalization was reduced in cells treated with CK-666 (C), EHT-1864 (D) or IPA-3 (E). (F,G) Quantification of results shown in A–E, evaluating all cortical endosomes (F) or focussing on cortical endosomes adjacent to the bottom membrane (G). (H) EHT-1864 treatment reduces the uptake of His-tagged IL-4Rα or IL-2Rγ by cells subjected to a pulse–chase labelling experiment with trisNTA–Alexa-Fluor-647 into cortical endosomes. Arrowheads indicate position of selected cortical endosomes. Error bars indicate s.d.

cortical endosomes formed upon overexpression of IL-2Rγ and JAK3–eGFP, our estimate of the concentration factor is conservative; in cells with exceptionally high expression levels, visible levels of receptor subunits tend to uniformly accumulate at the plasma membrane, indicating saturation of the endocytic machinery. Thus, the concentration factor we derived will, if anything, underestimate the true concentration step achieved by the cells at the lower endogenous receptor densities.

Journal of Cell Science

Journal of Cell Science (2015) 128, 3781-3795 doi:10.1242/jcs.170969

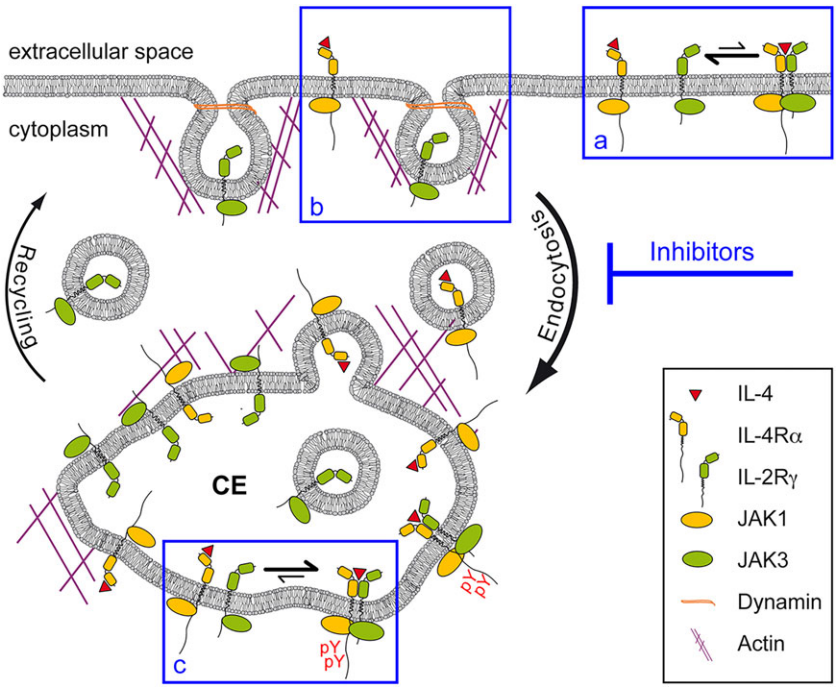

Fig. 8. The role of endocytosis in IL-4R signal transduction. (a) Low lateral affinities between IL-4R subunits prevent ligand-induced dimerization at the plasma membrane. (b) Receptors are continuously internalized by constitutive actin- and dynamin-mediated endocytosis. (c) The relative rates of endocytosis and recycling lead to an increased receptor density at the cortical endosome limiting membrane, which locally shifts the equilibrium towards receptor heterodimerization. Endocytosis is thus required for downstream signal transduction to compensate for the low, intrinsic affinities governing receptor complex formation. CE, cortical endosome.

Second, the dimerization behaviour of the different receptor complexes as observed by FLIM–FRET microscopy is consistent with the corresponding FCCS affinity measurements. Overexpression levels in our HEK293T model (200–300 receptors per μm^2) (Gandhi et al., 2014) are still below the two-dimensional dissociation constant for the low-affinity type 1 receptor complexes ($K_{d,2D}$≈1000 receptors per μm^2) (Gandhi et al., 2014). Consistent with this, in our FLIM experiments, these receptors exhibit a comparatively weak life time shift at the plasma membrane, and effective IL-4-induced formation of type 1 receptor complexes is largely confined to the cortical endosomes. In contrast, for type 2 IL-4R, these plasma membrane expression levels lie at or above the dissociation constant of the IL-4-induced heterodimers ($K_{d,2D}$≈180 receptors per μm^2). Correspondingly, we could also readily detect type 2 complex formation by FLIM at the plasma membrane.

Third, phosphorylated active IL-4R pathway components (IL-4Rα, JAK1 and JAK3) are enriched at the cortical endosomes following ligand exposure, suggesting that the cortical endosomes are the site of IL-4R-mediated JAK/STAT signal transduction. Cortical endosomes share certain properties with signalling endosomes of other pathways. Like the signalling compartments described for the Trk, neurothrophin (Valdez et al., 2007) and bone morphogenic protein (BMP) pathways (Bökel et al., 2006), cortical endosomes are Rab5- and EEA1-positive multivesicular endosomes. In addition, BMP signalling endosomes and cortical endosomes share the endosomal adaptor protein SARA (Bökel et al., 2006).

However, there are also clear differences: in most pathways, receptor uptake into signalling endosomes is a consequence of pathway activation, as exemplified by the TGF-β and RTK pathways (Bökel and Brand, 2014; Platta and Stenmark, 2011). Clearly this would not work if endocytosis were required upstream of receptor dimerization. Consistently, both steady state enrichment of the IL-2Rγ–JAK3 complexes at the cortical endosomes and internalization of IL-4Rα to cortical endosomes containing its heterodimerizing partners, IL-2Rγ or IL-13Rα1, occur constitutively in unstimulated cells, even with kinase-dead JAK3 versions.

Finally, inhibition of Rac-, Pak- and actin-mediated endocytosis reversibly blocks JAK/STAT signalling through all three IL-4R–ligand complexes, both at endogenous expression levels and under the overexpression conditions of our reconstitution system. This places endocytosis unambiguously upstream of signalling. Inhibition of signalling by CK-666 (Hetrick et al., 2013), which specifically affects the actin-branching factor Arp2, implicates the actin-organizing role of the Rac1 and Pak1 cassette in this process. We also tested several acting-stabilizing and -disassembling compounds (Phalloidin, Latrunculin A, cytochalasin D) for effects on STAT6 phosphorylation, but were unable to identify dosage windows where the observed effects were robust and reversible. Nevertheless, in pulse–chase experiments, inhibition of the Rac1-, Pak- and actin-mediated endocytosis reduced the internalization of both ligand and receptors to the cortical endosomes, consistent with the notion that the block in signalling is caused by reducing the endosomal density of occupied and recruited subunits.

Given that the IL-2Rγ subunit is known to interact with regulators of the endocytosis machinery (Basquin et al., 2013), it is likely that cortical endosomes are increased in size relative to the endogenous situation. In addition, local re-recruitment of the actin-branching machinery to the overexpressed IL-2Rγ chains, as reflected by the presence of phosphorylated Vav and Arp2/3, might cause extended retention of the cortical endosomes in the actin cortex, which could account for the presence of Rab11 in the periphery. The low physiological receptor levels prevented the characterization of the corresponding endogenous signalling compartment. Nevertheless, our inhibitor experiments unambiguously demonstrate that signalling through the endogenous type 1 and type 2 IL-4R complexes also requires Rac- and Pak-mediated endocytosis.

As yet, it remains unclear how widely this mechanism applies to other CKRs. Indeed, different processes may be used to subcellularly concentrate the various receptors, including clustering into lipid rafts or membrane associated signalosomes as reported for the IL-7R (Rose et al., 2010; Tamarit et al., 2013) and the IL-2R (Pillet et al., 2010) systems. However, membrane

Journal of Cell Science

Journal of Cell Science (2015) 128, 3781-3795 doi:10.1242/jcs.170969

partitioning and endocytosis need not be exclusive, since at least for the IL-2R subunits sorting into lipid ordered domains is thought to precede internalization (Lamaze et al., 2001). The increased local density of IL-2Rγ/JAK3 complexes observed in the plasma membrane immediately adjacent to the cortical endosomes relative to more distant regions may reflect the presence of such a mechanism also in the IL-4 system.

Importantly, the link between receptor endocytosis and pathway activation we describe for IL-4R might extend at least to the other common γ-chain-using CKRs; conditional knockouts of Rac1 and Rac2 (Dumont et al., 2009; Guo et al., 2008), Pak2 (Phee et al., 2014), and Vav1, Vav2 and Vav3 (Dumont et al., 2009; Fujikawa et al., 2003) exhibit a block in T-cell development at the $CD4^{-}$ $CD8^{-}$ stage that is currently attributed to various signalling pathways (e.g. Notch, Ras–MAPK and AKT) or defects in cytoskeletal organization and cell migration. However, this phenotype is surprisingly similar to the severe combined immunodeficiency caused by loss of IL-2Rγ, JAK3 or the IL-7R (O'Shea et al., 2004). A general requirement for Rac, Pak- and actin-mediated endocytosis in IL-2Rγ-associated CKR signalling would thus provide a more parsimonious explanation for this shared hematopoietic phenotype.

Combining low-affinity interactions between receptor subunits with constitutive endocytic enrichment in long-lived signalling endosomes allows cells to integrate weak extracellular signals over time and buffers these signals against temporal fluctuations. This might be especially useful for a receptor family largely associated with hematopoiesis and the regulation of immunity, where cells must respond to potentially distant and fluctuating cues. In addition, our inhibitor studies demonstrate that CKR signalling can in principle be targeted by interfering with receptor endocytosis through low molecular mass compounds. Our model therefore offers a new perspective for tackling diseases associated with excessive IL-4R activation, such as allergy and asthma.

MATERIALS AND METHODS

Molecular biology

Expression plasmids for pathway components have been described (Gandhi et al., 2014; Weidemann et al., 2011; Worch et al., 2010). pJAK3-R402H-eGFP and pJAK3-D949N-eGFP (Hofmann et al., 2004) were a gift from Sigrun Hofmann (Dresden University Children's Hospital, Dresden, Germany). pCMV6M-PAK1, pCMV6M-PAK1-K299R (Sells et al., 1997), pcDNA3-Rac1 and pCDNA3-Rac1T17N (Kraynov et al., 2000) were obtained from Addgene. pH6-IL4Rα-CyPet, pIL2Rγ-YPet, and pIL13Rα1-YPet were generated by inserting the CyPet and YPet open reading frames (Nguyen and Daugherty, 2005) into the respective receptor expression plasmids (Weidemann et al., 2011; Worch et al., 2010). All sequences are available upon request.

Cell culture

HEK293T cells were cultured in Dulbecco's modified Eagle's medium (DMEM; Gibco/Life Technologies, Darmstadt, Germany) with 10% fetal calf serum (FCS) and transfected with plasmids or esiRNA (Eupheria Biotech, Dresden, Germany) using Lipofectamine 2000 (Sigma-Aldrich, Taufkirchen, Germany) or Turbofect (Thermo Scientific, Bonn, Germany) in OptiMEM medium (Gibco). Jurkat cells were cultured in RPMI-1640 (Gibco) with 10% FCS and transfected using Turbofect. Cells were stimulated with 10 ng/ml IL-4 (Invitrogen/Life Technologies, Darmstadt, Germany) or 20 ng/ml IL-13 (Invitrogen).

Immunocytochemistry

Cells were processed as described previously (Kupinski et al., 2013). Primary antibodies were against: EEA1 (Abcam, Cambridge, UK, ab70521; mouse; 1:500), Arp2 H-84 (Santa Cruz Biotechnology, Santa Cruz, CA; sc-15389R; rabbit; 1:1000), phospho-Y497-IL-4Rα (Abcam; ab61099; rabbit; 1:1000), phospho-JAK1 (Santa Cruz; sc-16773R; rabbit; 1:1000), phospho-JAK3 (Santa Cruz Biotechnology, sc-16567R; rabbit; 1:1000), Rab5 (BD, Heidelberg, Germany; 610725; mouse; 1:1000), Rab11 (BD, 610657; mouse; 1:1000), Hrs (Acris, Herford, Germany; GTX101718; rabbit; 1:1000); phospho-Vav2 (Santa Cruz Biotechnology; sc-16409-R; rabbit; 1:1000), SARA (Abcam ab124875; rabbit; 1:1000); Alexa-Fluor-568–phalloidin (Invitrogen; 1:1000).

His tags were detected using trisNTA–Alexa-Fluor-647 (Lata et al., 2006) as described previously (Gandhi et al., 2014).

Imaging was performed on a Zeiss 780 confocal LSM. For object-based colocalization analysis colour channels were separately thresholded and regions of overlap between the resulting bitmap images quantified using Fiji or ImageJ software (Schindelin et al., 2012). Pixel-wise colocalization analysis was performed by Manders analysis using the automated thresholding functionality of the JaCoP Fiji and ImageJ plugin (Bolte and Cordelieres, 2006).

Immunoblots and inhibitor treatments

Cells pre-treated for 20 min in medium containing DMSO (up to 2%) or endocytosis inhibitors (chlorpromazine, up to 10 µM; dynasore, up to 400 µM; EHT-1864, up to 60 µM; IPA-3, up to 20 µM; CK-666, up to 400 µM; concentrations were retested batchwise and used as indicated) were stimulated with IL-4 or IL-13 (Gibco) at 37°C for 30 min in presence of compound. To test reversibility, cells were allowed to recover for 30 min in medium under continuous stimulation. Immunoblots were performed as described previously (Gandhi et al., 2014) with antibodies against phospho-STAT6 (Santa Cruz Biotechnology; sc-101808; rabbit; 1:200), STAT6 (Santa Cruz Biotechnology; sc-981; rabbit or mouse; 1:400) and GAPDH (Abcam; ab8245; mouse; 1:4000) antisera.

STAT6 phosphorylation and protein levels were quantified from band intensities (ImageQuant, GE Healthcare) and IC_{50} values calculated by fitting with a dose–response function

$$y = A_1 + \frac{A_2 - A_1}{1 + 10^{(\mathrm{IC}_{50} - c)p}}$$

where A_1, A_2 and p are descriptive parameters and c the varied inhibitor concentration (Origin 9.1, OriginLab).

Loading assays

Transferrin uptake was assayed by incubating cells with 20 µg/ml Rhodamin– or Alexa-Fluor-647–transferrin (Life Technologies) for 10 min at 4°C. After washing, cells were transferred to 37°C under continued presence of inhibitors (30 min) before acid stripping (150 mM NaCl and 100 mM glycin, pH 2.5), fixation and imaging.

IL-4–biotin was produced with the EZ-Link Sulfo-NHS-Biotinylation Kit (Thermo Scientific) according to instructions and cells loaded on ice (10 min) and incubated at 37°C (30 min).

IL-4 loading was quantified using a site specifically labelled IL-4–Alexa-Fluor-647 (Duppatla et al., 2014) (gift from Walter Sebald, Würzburg, Germany). HEK293T cells expressing IL-4Rα, and H6-IL-2Rγ and JAK3–eGFP were pre-incubated with inhibitors in culture medium at 37°C (15 min) and labelled on ice with 1 nM IL-4–Alexa-Fluor-647 (10 min). After washing, endocytosis was released in the presence of inhibitor at 37°C (20 min). For quantification, cells were imaged (LSM780, Zeiss) at three different planes using the GaAsP detector in integration mode. For image analysis (ImageJ), cortical endosomes were selected in the GFP channel by thresholding and the region of interest (ROI) measured in the Alexa Fluor 647 channel to determine area (A_k) and mean intensity (I_k) for a single cell in each frame (k). The total intensity per endosome (I_{endo}) was calculated by:

$$\langle I_{\mathrm{endo}} \rangle = \frac{\sum_k \langle I_k \rangle A_k}{\sum_k A_k} = \frac{\sum_k \langle I_k \rangle \langle A_{\mathrm{endo}} \rangle N_{\mathrm{endo}}}{\sum_k A_k},$$

where the average area per endosome A_{endo}=0.67 µm^2 was determined independently in the DMSO control to derive the number of endosomes in

Journal of Cell Science

each frame (N_{endo}). For statistics, we calculated the variance of the weighted sample mean:

$$\sigma = \left(\sum_k \left(\langle I_k \rangle - \langle I_{endo} \rangle \right)^2 w_k^2 \right)^{1/2} \text{ with } w_k = A_k / \sum_k A_k,$$

where w_k represent the weights accounting for the different number of endosomes per cell.

FLIM and FRET

FLIM measurements were performed on a Nikon TE-2000 microscope (Nikon, Tokyo, Japan) equipped with a 60×, NA 1.49 TIRF lens, a Becker and Hickl (Berlin, Germany) FLIM setup (DCS-120 scanner, PMC-100 high-speed PMT detector, Simple-Tau-152-DX time-correlated single photon counter), and a cooled laser diode module (445±5 nm, full width at half maximum 60–90 ps for 0.5 mW, 50 MHz).

Measurements were performed in air buffer at 22°C. 128×128 pixel images were scanned with a pixel dwell time of 11.55 µs and a pixel distance of 0.33 µm. Photon arrival times for individual pixels were fitted offline with a single exponential (binning 3, threshold 20 photons and fit range 1.5–13 ns). For each cell, donor lifetimes were separately averaged for five positions at the plasma membrane and five cortical endosomes identified by comparing the donor lifetime image with a fluorescence image in the acceptor channel.

Electron microscopy

Cells were processed for Tokuyasu cryosectioning and immunogold labelling as described previously (Slot and Geuze, 2007). 70-nm sections were cut on a Leica UC6+FC6 cryo-ultramicrotome and picked up in methyl cellulose with sucrose (2% methyl cellulose, Sigma M-6385, and 2.3 M sucrose, 1:1). The grids were incubated with primary antibodies (rabbit anti-GFP antibody, TP 401, Torrey Pines, 1:100; rabbit anti-biotin antibody, Enzo 43881, 1:100) followed by protein A conjugated to 10-nm gold particles, post-fixed in 1% glutaraldehyde and contrasted by incubation in methyl cellulose containing 0.4% uranylacetate. Alternatively, the primary anti-GFP antibody was detected with secondary antibodies coupled to ultra small gold particles (Aurion,~1 nm) followed by silver enhancement using the R-Gent SE/Kit (Aurion) before contrasting. For CLEM, ultrathin cryosections were labelled with chicken anti-GFP antibody (Abcam; ab13970), mouse anti-actin antibody (Cedarlane CLT 9001), rabbit anti-mouse-IgG antibody, protein A conjugated to 10-nm gold particles, and goat-anti-chicken-IgG conjugated to Alexa Fluor 488 as described previously (Fabig et al., 2012). Sections were analysed on a Philips Morgagni 268 TEM (FEI) at 80 kV.

Statistics

Data were plotted using box-and-whisker plots or as mean±s.d. column charts. Differences were tested for significance using Student's *t*-test for pairwise comparisons and ANOVA followed by Tukey's HSD post-hoc test for multiple comparisons. All data sets were measured at least in triplicate.

Acknowledgements

We thank John J. O'Shea and Sigrun Hofmann for providing JAK3 constructs and K. Crell, S. Herrmann, S. Knappe, S. von Kannen, R. Perez Palencia, S. Kretschmar, and S. Lange for technical assistance. T.W. is grateful to Walter Sebald and Eugene Petrov for inspiring discussions.

Competing interests

The authors declare no competing or financial interests.

Author contributions

T.W. discovered cortical endosomes and initiated the experiments, T.W. and C.B. devised the experimental strategy, K.K. and T.W. performed pharmacological studies, H.G. and K.K. characterized the endosomes, T.K. and H.G. performed the EM analysis, S.P. and C.B. performed FLIM and FRET experiments, P.S., T. W. and C.B. were responsible for data interpretation, T.W. and C.B. wrote the manuscript.

Funding

This work was supported by a Center for Regenerative Therapies Dresden (CRTD) seed grant (to K.K., C.B., P.S. and T.W.); and Deutsche Forschungsgemeinschaft (DFG) priority program TRR 67 (to H.G., T.W. and P.S.).

Supplementary information

Supplementary information available online at http://jcs.biologists.org/lookup/suppl/doi:10.1242/jcs.170969/-/DC1

References

Bache, K. G., Brech, A., Mehlum, A. and Stenmark, H. (2003). Hrs regulates multivesicular body formation via ESCRT recruitment to endosomes. *J. Cell Biol.* **162**, 435-442.

Basquin, C., Malarde, V., Mellor, P., Anderson, D. H., Meas-Yedid, V., Olivo-Marin, J.-C., Dautry-Varsat, A. and Sauvonnet, N. (2013). The signalling factor PI3K is a specific regulator of the clathrin-independent dynamin-dependent endocytosis of IL-2 receptors. *J. Cell Sci.* **126**, 1099-1108.

Bökel, C. and Brand, M. (2014). Endocytosis and signaling during development. *Cold Spring Harb. Perspect. Biol.* **6**, a017020.

Bökel, C., Schwabedissen, A., Entchev, E., Renaud, O. and Gonzalez-Gaitan, M. (2006). Sara endosomes and the maintenance of Dpp signaling levels across mitosis. *Science* **314**, 1135-1139.

Bolte, S. and Cordelières, F. P. (2006). A guided tour into subcellular colocalization analysis in light microscopy. *J. Microsc.* **224**, 213-232.

Boucrot, E., Ferreira, A. P. A., Almeida-Souza, L., Debard, S., Vallis, Y., Howard, G., Bertot, L., Sauvonnet, N. and McMahon, H. T. (2014). Endophilin marks and controls a clathrin-independent endocytic pathway. *Nature* **517**, 460-465.

Boulay, J.-L., O'Shea, J. J. and Paul, W. E. (2003). Molecular phylogeny within type I cytokines and their cognate receptors. *Immunity* **19**, 159-163.

Constantinescu, S. N., Keren, T., Socolovsky, M., Nam, H.-s., Henis, Y. I. and Lodish, H. F. (2001). Ligand-independent oligomerization of cell-surface erythropoietin receptor is mediated by the transmembrane domain. *Proc. Natl. Acad. Sci. USA* **98**, 4379-4384.

Deacon, S. W., Beeser, A., Fukui, J. A., Rennefahrt, U. E. E., Myers, C., Chernoff, J. and Peterson, J. R. (2008). An isoform-selective, small-molecule inhibitor targets the autoregulatory mechanism of p21-activated kinase. *Chem. Biol.* **15**, 322-331.

Di Guglielmo, G. M., Baass, P. C., Ou, W. J., Posner, B. I. and Bergeron, J. J. (1994). Compartmentalization of SHC, GRB2 and mSOS, and hyperphosphorylation of Raf-1 by EGF but not insulin in liver parenchyma. *EMBO J.* **13**, 4269-4277.

Di Guglielmo, G. M., Le Roy, C., Goodfellow, A. F. and Wrana, J. L. (2003). Distinct endocytic pathways regulate TGF-beta receptor signalling and turnover. *Nat. Cell Biol.* **5**, 410-421.

Dumont, C., Corsoni-Tadrzak, A., Ruf, S., de Boer, J., Williams, A., Turner, M., Kioussis, D. and Tybulewicz, V. L. (2009). Rac GTPases play critical roles in early T-cell development. *Blood* **113**, 3990-3998.

Duppatla, V., Gjorgjevikj, M., Schmitz, W., Hermanns, H. M., Schäfer, C. M., Kottmair, M., Müller, T. and Sebald, W. (2014). IL-4 analogues with site-specific chemical modification at position 121 inhibit IL-4 and IL-13 biological activities. *Bioconjug. Chem.* **25**, 52-62.

Fabig, G., Kretschmar, S., Weiche, S., Eberle, D., Ader, M. and Kurth, T. (2012). Labeling of ultrathin resin sections for correlative light and electron microscopy. *Methods Cell Biol.* **111**, 75-93.

Friedrich, K., Kammer, W., Erhardt, I., Brandlein, S., Arnold, S. and Sebald, W. (1999). The two subunits of the interleukin-4 receptor mediate independent and distinct patterns of ligand endocytosis. *Eur. J. Biochem.* **265**, 457-465.

Fujikawa, K., Miletic, A. V., Alt, F. W., Faccio, R., Brown, T., Hoog, J., Fredericks, J., Nishi, S., Mildiner, S., Moores, S. L. et al. (2003). Vav1/2/3-null mice define an essential role for Vav family proteins in lymphocyte development and activation but a differential requirement in MAPK signaling in T and B cells. *J. Exp. Med.* **198**, 1595-1608.

Gandhi, H., Worch, R., Kurgonaite, K., Hintersteiner, M., Schwille, P., Bökel, C. and Weidemann, T. (2014). Dynamics and interaction of interleukin-4 receptor subunits in living cells. *Biophys. J.* **107**, 2515-2527.

Grassart, A., Dujeancourt, A., Lazarow, P. B., Dautry-Varsat, A. and Sauvonnet, N. (2008). Clathrin-independent endocytosis used by the IL-2 receptor is regulated by Rac1, Pak1 and Pak2. *EMBO Rep.* **9**, 356-362.

Grassart, A., Meas-Yedid, V., Dufour, A., Olivo-Marin, J.-C., Dautry-Varsat, A. and Sauvonnet, N. (2010). Pak1 phosphorylation enhances cortactin-N-WASP interaction in clathrin-caveolin-independent endocytosis. *Traffic* **11**, 1079-1091.

Grimes, M. L., Zhou, J., Beattie, E. C., Yuen, E. C., Hall, D. E., Valletta, J. S., Topp, K. S., LaVail, J. H., Bunnett, N. W. and Mobley, W. C. (1996). Endocytosis of activated TrkA: evidence that nerve growth factor induces formation of signaling endosomes. *J. Neurosci.* **16**, 7950-7964.

Guo, F., Cancelas, J. A., Hildeman, D., Williams, D. A. and Zheng, Y. (2008). Rac GTPase isoforms Rac1 and Rac2 play a redundant and crucial role in T-cell development. *Blood* **112**, 1767-1775.

Journal of Cell Science

Hage, T., Sebald, W. and Reinemer, P. (1999). Crystal structure of the interleukin-4/receptor alpha chain complex reveals a mosaic binding interface. *Cell* **97**, 271-281.
Hetrick, B., Han, M. S., Helgeson, L. A. and Nolen, B. J. (2013). Small molecules CK-666 and CK-869 inhibit actin-related protein 2/3 complex by blocking an activating conformational change. *Chem. Biol.* **20**, 701-712.
Hinterleitner, C., Huelsenbeck, J., Henninger, C., Wartlick, F., Schorr, A., Kaina, B. and Fritz, G. (2013). Rac1 signaling protects monocytic AML cells expressing the MLL-AF9 oncogene from caspase-mediated apoptotic death. *Apoptosis* **18**, 963-979.
Hofmann, S. R., Lam, A. Q., Frank, S., Zhou, Y.-J., Ramos, H. L., Kanno, Y., Agnello, D., Youle, R. J. and O'Shea, J. J. (2004). Jak3-independent trafficking of the common gamma chain receptor subunit: chaperone function of Jaks revisited. *Mol. Cell. Biol.* **24**, 5039-5049.
Kagan, J. C., Su, T., Horng, T., Chow, A., Akira, S. and Medzhitov, R. (2008). TRAM couples endocytosis of Toll-like receptor 4 to the induction of interferon-beta. *Nat. Immunol.* **9**, 361-368.
Kraynov, V. S., Chamberlain, C., Bokoch, G. M., Schwartz, M. A., Slabaugh, S. and Hahn, K. M. (2000). Localized Rac activation dynamics visualized in living cells. *Science* **290**, 333-337.
Kupinski, A. P., Raabe, I., Michel, M., Ail, D., Brusch, L., Weidemann, T. and Bökel, C. (2013). Phosphorylation of the Smo tail is controlled by membrane localisation and is dispensable for clustering. *J. Cell Sci.* **126**, 4684-4697.
Lamaze, C., Dujeancourt, A., Baba, T., Lo, C. G., Benmerah, A. and Dautry-Varsat, A. (2001). Interleukin 2 receptors and detergent-resistant membrane domains define a clathrin-independent endocytic pathway. *Mol. Cell* **7**, 661-671.
LaPorte, S. L., Juo, Z. S., Vaclavikova, J., Colf, L. A., Qi, X., Heller, N. M., Keegan, A. D. and Garcia, K. C. (2008). Molecular and structural basis of cytokine receptor pleiotropy in the interleukin-4/13 system. *Cell* **132**, 259-272.
Lata, S., Gavutis, M., Tampé, R. and Piehler, J. (2006). Specific and stable fluorescence labeling of histidine-tagged proteins for dissecting multi-protein complex formation. *J. Am. Chem. Soc.* **128**, 2365-2372.
Leonard, W. J. and O'Shea, J. J. (1998). Jaks and STATs: biological implications. *Annu. Rev. Immunol.* **16**, 293-322.
Lowenthal, J. W., Castle, B. E., Christiansen, J., Schreurs, J., Rennick, D., Arai, N., Hoy, P., Takebe, Y. and Howard, M. (1988). Expression of high affinity receptors for murine interleukin 4 (BSF-1) on hemopoietic and nonhemopoietic cells. *J. Immunol.* **140**, 456-464.
Macia, E., Ehrlich, M., Massol, R., Boucrot, E., Brunner, C. and Kirchhausen, T. (2006). Dynasore, a cell-permeable inhibitor of dynamin. *Dev. Cell* **10**, 839-850.
Manders, E. M. M., Verbeek, F. J. and Aten, J. A. (1993). Measurement of co-localization of objects in dual-colour confocal images. *J. Microsc.* **169**, 375-382.
Miaczynska, M., Pelkmans, L. and Zerial, M. (2004). Not just a sink: endosomes in control of signal transduction. *Curr. Opin. Cell Biol.* **16**, 400-406.
Murata, T., Taguchi, J. and Puri, R. K. (1998). Interleukin-13 receptor alpha' but not alpha chain: a functional component of interleukin-4 receptors. *Blood* **91**, 3884-3891.
Nelms, K., Keegan, A. D., Zamorano, J., Ryan, J. J. and Paul, W. E. (1999). The IL-4 receptor: signaling mechanisms and biologic functions. *Annu. Rev. Immunol.* **17**, 701-738.
Nguyen, A. W. and Daugherty, P. S. (2005). Evolutionary optimization of fluorescent proteins for intracellular FRET. *Nat. Biotechnol.* **23**, 355-360.
Ohara, J. and Paul, W. E. (1987). Receptors for B-cell stimulatory factor-1 expressed on cells of haematopoietic lineage. *Nature* **325**, 537-540.
O'Shea, J. J., Husa, M., Li, D., Hofmann, S. R., Watford, W., Roberts, J. L., Buckley, R. H., Changelian, P. and Candotti, F. (2004). Jak3 and the pathogenesis of severe combined immunodeficiency. *Mol. Immunol.* **41**, 727-737.
Park, L. S., Friend, D., Sassenfeld, H. M. and Urdal, D. L. (1987). Characterization of the human B cell stimulatory factor 1 receptor. *J. Exp. Med.* **166**, 476-488.
Phee, H., Au-Yeung, B. B., Pryshchep, O., O'Hagan, K. L., Fairbairn, S. G., Radu, M., Kosoff, R., Mollenauer, M., Cheng, D., Chernoff, J. et al. (2014). Pak2 is required for actin cytoskeleton remodeling, TCR signaling, and normal thymocyte development and maturation. *Elife* **3**, e02270.
Pillet, A.-H., Lavergne, V., Pasquier, V., Gesbert, F., Thèze, J. and Rose, T. (2010). IL-2 induces conformational changes in its preassembled receptor core, which then migrates in lipid raft and binds to the cytoskeleton meshwork. *J. Mol. Biol.* **403**, 671-692.
Platta, H. W. and Stenmark, H. (2011). Endocytosis and signaling. *Curr. Opin. Cell Biol.* **23**, 393-403.
Rose, T., Pillet, A.-H., Lavergne, V., Tamarit, B., Lenormand, P., Rousselle, J.-C., Namane, A. and Thèze, J. (2010). Interleukin-7 compartmentalizes its receptor signaling complex to initiate CD4T lymphocyte response. *J. Biol. Chem.* **285**, 14898-14908.
Sauvonnet, N., Dujeancourt, A. and Dautry-Varsat, A. (2005). Cortactin and dynamin are required for the clathrin-independent endocytosis of gammac cytokine receptor. *J. Cell Biol.* **168**, 155-163.
Schindelin, J., Arganda-Carreras, I., Frise, E., Kaynig, V., Longair, M., Pietzsch, T., Preibisch, S., Rueden, C., Saalfeld, S., Schmid, B. et al. (2012). Fiji: an open-source platform for biological-image analysis. *Nat. Methods* **9**, 676-682.
Sells, M. A., Knaus, U. G., Bagrodia, S., Ambrose, D. M., Bokoch, G. M. and Chernoff, J. (1997). Human p21-activated kinase (Pak1) regulates actin organization in mammalian cells. *Curr. Biol.* **7**, 202-210.
Shutes, A., Onesto, C., Picard, V., Leblond, B., Schweighoffer, F. and Der, C. J. (2007). Specificity and mechanism of action of EHT 1864, a novel small molecule inhibitor of Rac family small GTPases. *J. Biol. Chem.* **282**, 35666-35678.
Sigismund, S., Argenzio, E., Tosoni, D., Cavallaro, E., Polo, S. and Di Fiore, P. P. (2008). Clathrin-mediated internalization is essential for sustained EGFR signaling but dispensable for degradation. *Dev. Cell* **15**, 209-219.
Slot, J. W. and Geuze, H. J. (2007). Cryosectioning and immunolabeling. *Nat. Protoc.* **2**, 2480-2491.
Subtil, A., Hemar, A. and Dautry-Varsat, A. (1994). Rapid endocytosis of interleukin 2 receptors when clathrin-coated pit endocytosis is inhibited. *J. Cell Sci.* **107**, 3461-3468.
Tamarit, B., Bugault, F., Pillet, A. H., Lavergne, V., Bochet, P., Garin, N., Schwarz, U., Theze, J. and Rose, T. (2013). Membrane microdomains and cytoskeleton organization shape and regulate the IL-7 receptor signalosome in human CD4 T-cells. *J. Biol. Chem.* **288**, 8691-8701.
Tsukazaki, T., Chiang, T. A., Davison, A. F., Attisano, L. and Wrana, J. L. (1998). SARA, a FYVE domain protein that recruits Smad2 to the TGFbeta receptor. *Cell* **95**, 779-791.
Valdez, G., Philippidou, P., Rosenbaum, J., Akmentin, W., Shao, Y. and Halegoua, S. (2007). Trk-signaling endosomes are generated by Rac-dependent macroendocytosis. *Proc. Natl. Acad. Sci. USA* **104**, 12270-12275.
Vieira, A. V., Lamaze, C. and Schmid, S. L. (1996). Control of EGF receptor signaling by clathrin-mediated endocytosis. *Science* **274**, 2086-2089.
Wang, L. H., Rothberg, K. G. and Anderson, R. G. (1993). Mis-assembly of clathrin lattices on endosomes reveals a regulatory switch for coated pit formation. *J. Cell Biol.* **123**, 1107-1117.
Weidemann, T., Höfinger, S., Müller, K. and Auer, M. (2007). Beyond dimerization: a membrane-dependent activation model for interleukin-4 receptor-mediated signalling. *J. Mol. Biol.* **366**, 1365-1373.
Weidemann, T., Worch, R., Kurgonaite, K., Hintersteiner, M., Bökel, C. and Schwille, P. (2011). Single cell analysis of ligand binding and complex formation of interleukin-4 receptor subunits. *Biophys. J.* **101**, 2360-2369.
Whitty, A. and Riera, T. V. (2008). New ways to target old receptors. *Curr. Opin. Chem. Biol.* **12**, 427-433.
Worch, R., Bökel, C., Höfinger, S., Schwille, P. and Weidemann, T. (2010). Focus on composition and interaction potential of single-pass transmembrane domains. *Proteomics* **10**, 4196-4208.
Zhang, J.-L., Buehner, M. and Sebald, W. (2002a). Functional epitope of common gamma chain for interleukin-4 binding. *Eur. J. Biochem.* **269**, 1490-1499.
Zhang, J.-L., Simeonowa, I., Wang, Y. and Sebald, W. (2002b). The high-affinity interaction of human IL-4 and the receptor alpha chain is constituted by two independent binding clusters. *J. Mol. Biol.* **315**, 399-407.